Biomimetic Surface Modification of Honeycomb Films via a "Grafting From" Approach

ARTICLE *in* LANGMUIR · AUGUST 2010

Impact Factor: 4.46 · DOI: 10.1021/la1011567 · Source: PubMed

Langmuir
Article
pubs.acs.org/Langmuir

Biomimetic Surface Modification of Honeycomb Films via a "Grafting From" Approach

Daniel Nyström,[†] Eva Malmström,[†] Anders Hult,[†] Idriss Blakey,[‡] Cyrille Boyer,[§] Thomas P. Davis,*[,§] and Michael R. Whittaker*[,§]

[†]*Fiber and Polymer Technology, KTH, Teknikringen 56-58, SE-100 44 Stockholm, Sweden,* [‡]*Australian Institute for Bioengineering and Nanotechnology and Centre for Advanced Imaging, The University of Queensland, QLD. 4072, Brisbane, Australia, and* [§]*Centre for Advanced Macromolecular Design (CAMD), School of Chemical Engineering, The University of New South Wales, Sydney, NSW, Australia 2052*

Received March 24, 2010. Revised Manuscript Received June 15, 2010

Hydrophobic isoporous membranes were fabricated using the "breath figure" method from polystyrene stars synthesized via ATRP. The living polymer chain ends at the surface of the films were then used, without further modification, in a "grafting-from" approach to grow surface-linked polyglycidyl methacrylate chains under conditions that maintained the regular honeycomb structure. This versatile functional surface was then used as a platform to build a small library of surfaces using a variety of simple chemistries: (i) the acid hydrolysis of the epoxide to form bis-alcohol groups and (ii) utilizing the "click-like" epoxide−amine reaction to functionalize the surface with a model biomolecule—(biotinamido)pentylamine. The successful modifications were confirmed by a combination of spectroscopic and biological means. Changes in the growth characteristics of nonmotile *Psychrobacter* sp. strain, SW5, on the honeycomb films, provided further evidence confirming changes in the hydrophobicity of the surface upon grafting.

Introduction

The ability to precisely design and control the properties of polymer surfaces is of critical importance in their use in many biomedical applications; these range from implants to bioassay substrates.[1−3] It has been demonstrated widely that both the physical morphology of a film at the nano- and/or microlevel and the inherent chemistry of a film's surface will be important in determining their performance in vitro and in vivo. For example, polymeric materials that are in contact with complex biological fluids have faced critical problems, such as undesirable protein adsorption and cell adhesion due to poor biocompatibility of the surface leading to undesirable immunological responses.[4]

The "breath figure" method is one of the most facile approaches to polymer films with controlled micro- and nanoscale features: honeycomb films. First described by Francois et al.,[5−8] this method involves a simple casting of polymer films from appropriate solvents in a humid atmosphere. The result is a polymer film with either interconnected or isolated, hexagonally close-packed pore morphology, formed via a self-organizing process of the polymer around condensing water droplets that form on the surface.[9−14] These surface and bulk features can be routinely controlled by optimizing the casting conditions, such as the air flow,[15] the nature and the density of solvent used for the casting,[16−18] and the polymer architecture and casting concentration.

The original work on breath figures published by Francois et al.[5−8] was based on star polymers of polystyrene made by anionic polymerization, and initial experiments performed in the CAMD laboratories in the late 1990s also focused on similar polymers. The advent of living radical polymerization (LRP)[19−23] provided the opportunity to apply LRP to make novel structures for breath figure casting, and in early papers, both RAFT and metal-mediated polymerization were used to make star architectures[24−26] and later different architectures (such as microgels, blocks, and combs) and

*Corresponding authors. E-mail: T.Davis@unsw.edu.au (T.P.D.); mikey.whittaker@unsw.edu.au (M.R.W.).

(1) Chong, M. S. K.; Chan, J.; Choolani, M.; Lee, C.-N.; Teoh, S.-H. *Biomaterials* **2009**, *30*, 2241–2251.
(2) He, D.; Sun, W.; Schrader, T.; Ulbricht, M. *J. Mater. Chem.* **2009**, *19*, 253–260.
(3) Murthy, R.; Shell, C. E.; Grunlan, M. A. *Biomaterials* **2009**, *30*, 2433–2439.
(4) Kato, K.; Uchida, E.; Kang, E.-T.; Uyama, Y.; Ikada, Y. *Prog. Polym. Sci.* **2002**, *28*, 209–259.
(5) Francois, B.; Ederle, Y.; Mathis, C. *Synth. Met.* **1999**, *103*, 2362–2363.
(6) Francois, B.; Pitois, O.; Francois, J. *Adv. Mater.* **1995**, *7*, 1041–1044.
(7) Francois, B.; Widawski, G.; Rawiso, M.; Cesar, B. *Synth. Met.* **1995**, *69*, 463–466.
(8) Widawski, G.; Rawiso, M.; Francois, B. *Nature* **1994**, *369*, 387–389.
(9) Peng, J.; Han, Y.; Yang, Y.; Li, B. *Polymer* **2004**, *45*, 447–452.
(10) Karthaus, O.; Maruyama, N.; Cieren, X.; Shimomura, M.; Hasegawa, H.; Hashimoto, T. *Langmuir* **2000**, *16*, 6071–6076.
(11) Angus, S. D.; Davis, T. P. *Langmuir* **2002**, *18*, 9547–9553.
(12) Govor, L. V.; Bashmakov, I. A.; Kiebooms, R.; Dyakonov, V.; Parisi, J. *Adv. Mater.* **2001**, *13*, 588.
(13) Govor, L. V.; Bashmakov, I. A.; Kaputski, F. N.; Pientka, M.; Parisi, J. *Macromol. Chem. Phys.* **2000**, *201*, 2721.
(14) Bormashenko, E.; Malkin, A.; Musin, A.; Bormashenko, Y.; G., W.; Litvak, N.; Barkay, Z.; Machavariani, V. *Macromol. Chem. Phys.* **2008**, *209*, 567.
(15) Stenzel, M. H. *Aust. J. Chem.* **2002**, *55*, 239–243.
(16) Srinivasarao, M.; Collings, D.; Philips, A.; Patel, S. *Science* **2001**, *272*, 79.
(17) Tung, P.-H.; Huang, C.-F.; Chen, S.-C.; Hsu, C.-H.; Chang, F.-C. *Desalination* **2006**, *200*, 55–57.
(18) Tung, P.-H.; Kuo, S.-W.; Jeong, K.-U.; Cheng, S. Z. D.; Huang, C.-F.; Chang, F.-C. *Macromol. Rapid Commun.* **2007**, *28*, 271–275.
(19) Boyer, C.; Bulmus, V.; Davis, T. P.; Ladmiral, V.; Liu, J.; Perrier, S. *Chem. Rev.* **2009**, *109*, 5402–5436.
(20) Matyjaszewski, K.; Xia, J. *Chem. Rev.* **2001**, *101*, 2921–2990.
(21) Moad, G.; Rizzardo, E.; Thang, S. H. *Aust. J. Chem.* **2009**, *62*, 1402–1472.
(22) Hawker, C. J.; Bosman, A. W.; Harth, E. *Chem. Rev.* **2001**, *101*, 3661–3688.
(23) David, G.; Boyer, C.; Tonnar, J.; Ameduri, B.; Lacroix-Desmazes, P.; Boutevin, B. *Chem. Rev.* **2006**, *106*, 3936–3962.
(24) Stenzel, M. H.; Barner-Kowollik, C.; Davis, T. P. *J. Polym. Sci., Part A: Polym. Chem.* **2006**, *44*, 2363.
(25) Stenzel-Rosenbaum, M. H.; Davis, T. P.; Chen, V.; Fane, A. G. *Macromolecules* **2001**, *34*, 5433.
(26) Stenzel-Rosenbaum, M. H.; Davis, T. P.; Fane, A. G.; Chen, V. *Angew. Chem., Int. Ed.* **2001**, *40*, 3428–3432.

hybrid materials consisting of polystyrene-grafted silica nanoparticles.[27−31] Subsequently, CAMD work on honeycomb films was applied to biotechnology applications (in collaboration with industrial partners—see acknowledgments), leading to a number of patents based on grafting and cross-linking of the honeycomb films.[32−34]

The surface chemistry and surface topography are important factors that dictate how these honeycomb membranes perform in the biotechnology applications with both the morphology and surface chemistry playing a role in how living cells interact with these honeycomb surfaces. Yamamoto et al.[35] have demonstrated that compared to flat films breath figure patterned films (both modified with fibronectin) result in increased expression of focal adhesion kinase autophosphorylated at the tyrosine residue, a crucial signal transduction protein that mediates cell adhesion, growth, and proliferation. In terms of designing surfaces for bioassays, breath feature films have a high surface area, which results in a high number of potential points for functionalization, which can lead to higher sensitivities and lower detection limits. Another advantage of these porous surfaces is that deposition of materials can be more uniform because the "coffee ring" effect is alleviated for porous surfaces. This also can result in improved assay reliability.[36] Surprisingly, there have been relatively few publications describing control over the surface chemistry of honeycomb membranes.[24,26,37,38] To date, these surface modification approaches have utilized either the casting of inherently functional polymer materials or the chemical postmodification of the isoporous surface after casting.[39] Davis and Stenzel et al.[26,29,40,41] have described both of these approaches to yield functional macroporous films. However, it was found that in some instances the surface modification procedure could have a detrimental impact on the morphology of the film,[41] in some cases completely destroying the porous morphology and at best requiring a complete reoptimization of casting protocols.

One way to overcome surface modification limitations is to utilize surface specific functionalization techniques to introduce precise control over the surface of the isoporous films after casting.[24,41] The properties of the interface can therefore be tailored via chemical modification for specific applications without affecting the bulk properties of the film or requiring the reoptimization of casting conditions.

An alternative approach to surface modification is to access the inherent chain-end functionality of the polymers synthesized via a LRP at the films surface. In this approach the chain ends can be reinitiated from the surface in a traditional "bottom-up" surface grafting strategy to yield grafted polymer brushes.[39,42,43]

In the present study we aim to demonstrate a "bottom-up" approach to the surface modification of highly regular isoporous polystyrene honeycomb films using ATRP. Polystyrene stars synthesized via ATRP have been shown to give highly isoporous membranes with tunable morphologies.[26] An epoxide-containing functional monomer, glycidyl methacrylate (GMA), was chosen as a monomer of the surface grafted layer. ATRP of GMA under mild conditions has been reported by others,[44−47] and when used as a surface graft containing epoxide groups, it yields a versatile synthetic platform for further biorelevant chemical modifications,[27,48] for example, (i) the acid hydrolysis of the epoxide to form bis-alcohol groups[49] or (ii) reaction with nucleophiles (amines, alcohols, or thiols).[45,50−52]

Experimental Part

Materials. Copper(I) bromide (CuBr, 98%), d-chloroform (99.9%), 2,2′-dipyridyl (Bipy, 99%), 2-bromoisobutyryl bromide (98%), α-D-glucose, and chloroform (98%) were used as received from Aldrich. Styrene (99%) and glycidyl methacrylate (GMA, 97%) were also acquired from Aldrich but were deinhibited by running through a column of basic alumina oxide before use. AR grade pyridine and methanol were used as received from SDS; AR grade toluene and carbon disulfide (CS_2) were used as received from Univar. (Biotinamido)pentylamine and streptavidin-Cy5 were obtained from Pierce and were used as received.

Instrumental Characterization. *Nuclear Magnetic Resonance*. ^{1}H NMR spectra were recorded on a 300 MHz (Bruker ACF300) spectrometer using d-chloroform as solvent.

Optical Imaging. Film surface images were taken by reflectance microscopy on a coupled reflectance/transmittance optical microscope at various magnifications. Photos were taken with an Onyx digital camera and recorded via PicoloDigiCAm digital imaging software.

Fluorescent Imaging. Scanning confocal laser microscope images were obtained using an Olympus GB200 instrument (Olympus Optical Co. Ltd.) fitted with a piezoelectric z stage with a reproducibility of ± 0.2 μm. The microscope was equipped with a 60×, 1.4-numerical-aperture oil immersion lens. An argon laser with emission line at 488 nm was used as the excitation source for the rhodamine B fluorophore.

Size Exclusion Chromatography (*SEC*). SEC analyses were performed on a modular system comprised of a GBC LC1120 HPLC pump operating at room temperature, an in-line ERC-3415

(27) Nyström, D.; Lindqvist, J.; Östmark, E.; Hult, A.; Malmström, E. *Chem. Commun*. **2006**, 3594.
(28) Lord, H. T.; Quinn, J. F.; Angus, S. D.; Whittaker, M. R.; Stenzel, M. H.; Davis, T. P. *J. Mater. Chem*. **2003**, *13*, 2819–2824.
(29) Stenzel, M. H.; Davis, T. P.; Fane, A. G. *J. Mater. Chem*. **2003**, *13*, 2090–2097.
(30) Hao, X.; Stenzel, M. H.; Barner-Kowollik, C.; Davis, T. P.; Evans, E. *Polymer* **2004**, *45*, 7401–7415.
(31) Nyström, D.; Antoni, P.; Johansson, M.; Malmström, E.; Hult, A. *Macromol. Rapid Commun*. **2005**, *26*, 524–228.
(32) Stenzel-Rosenbaum, M. H.; Davis, T. World Patent 2002/050174, 2002 (Polymerat Pty Ltd., Australia).
(33) Rasoul, F.; Maeji, J.; Whittaker, M.; Kambouris, P.; Davis, T. World Patent 2003/040218, 2003 (Polymerat Pty Ltd., Australia).
(34) Kambouris, P.; Whittaker, M.; Davis, T.; Blakey, I.; Day, G. World Patent 2002/079305, 2002 (Polymerat Pty Ltd., Australia).
(35) Yamamoto, S.; Tanaka, M.; Sunami, H.; Ito, E.; Yamashita, S.; Morita, Y.; Shimomura, M. *Langmuir* **2007**, *23*, 8114–8120.
(36) Ressine, A.; Ekström, S.; Marko-Varga, G.; Laurell, T. *Anal. Chem*. **2003**, *75*, 6968–6974.
(37) Barner-Kowollik, C.; Dalton, H.; Davis, T. P.; Stenzel, M. H. *Angew. Chem., Int. Ed*. **2003**, *42*, 3664–3668.
(38) Yabu, H.; Hirai, Y.; Kojima, M.; Shimomura, M. *Chem. Mater*. **2009**, *21*, 1787–1789.
(39) Shimomura, M.; Sawadaishi, T. *Curr. Opin. Colloid Interface Sci*. **2001**, *6*, 11–16.
(40) Wong, K. H.; Davis, T. P.; Barner-Kowollik, C.; Stenzel, M. H. *Polymer* **2007**, *48*, 4950–4965.
(41) Stenzel, M. H.; Davis, T. P. *Aust. J. Chem*. **2003**, *56*, 1035–1038.
(42) Ma, I. Y.; Lobb, J. E.; Billingham, N. C.; Armes, S. P.; Lewis, A. L.; Lloyd, A. W.; Salvage, J. *Macromolecules* **2002**, *35*, 9306–9314.
(43) Ke, B.-B.; Wan, L.-S.; Xu, Z.-K. *Langmuir* **2010**, ASAP, DOI: 10.1021/la904729b.
(44) Cañamero, P. F.; Fuente, J. L. d. l.; Madruga, E. L.; Fernández-García, M. *Macromol. Chem. Phys*. **2004**, *205*, 2221–2228.
(45) Colomines, G.; Otazaghine, B.; Boyer, C.; Monge, S.; Robin, J.-J. *J. Polym. Sci., Part A: Polym. Chem*. **2008**, *46*, 433–443.
(46) Haloi, D. J.; Roy, S.; Singha, N. K. *J. Polym. Sci., Part A: Polym. Chem*. **2009**, *47*, 6526.
(47) de la Fuente, J. L.; Cañamero, P. F.; Fernández-García, M. *J. Polym. Sci., Part A: Polym. Chem*. **2006**, *44*, 1807–1816.
(48) Jonsson, M.; Nyström, D.; Nordin, O.; Malmström, E. *Eur. Polym. J*. **2009**, *45*, 2374–2382.
(49) Gudipati, C. S.; Tan, M. B. H.; Hussain, H.; Liu, Y.; He, C.; Davis, T. P. *Macromol. Rapid Commun*. **2008**, *29*, 1902–1907.
(50) Carioscia, J. A.; Stansbury, J. W.; Bowman, C. N. *Polymer* **2007**, *48*, 1526–1532.
(51) Grazu, V.; Abian, O.; Mateo, C.; Batista-Viera, F.; Fernandez-Lafuente, R.; Guisan, J. M. *Biotechnol. Bioeng*. **2005**, *90*, 597–605.
(52) Nystrom, D.; Lindqvist, J.; stmark, E.; Antoni, P.; Carlmark, A.; Hult, A.; Malmstrom, E. *ACS Appl. Mater. Interfaces* **2009**, *1*, 816–823.

degasser unit, a SIL-10AD VP Shimadzu autoinjector with a stepwise injection control meter with an accuracy of ±1 μL, a column set which consisted of a PL 5.0 μm bead size guard column and a set of 3 × 5.0 μm PL linear columns (10^3, 10^4, 10^5 Å), and an RI detector. Tetrahydrofuran was utilized as the continuous phase at a flow rate of 1 mL/min and a temperature of 40 °C. Linear polystyrene standards were used for calibration.

Attenuated Total Reflectance Infrared Spectroscopy (ATR-IR). Attenuated total reflectance−Fourier transform infrared (ATR-IR) spectra were obtained on a Nicolet Nexus 5700 FTIR spectrometer equipped with a Nicolet Smart Orbit single bounce, diamond ATR accessory (Thermo Electron Corp., Waltham, MA). Spectra were recorded at 4 cm^{-1} resolution for at least 32 scans with an optical path difference (OPD) velocity of 0.6289 cm s^{-1}. Solids were pressed directly onto the diamond internal reflection element of the ATR accessory without further sample preparation. Spectra were manipulated using the OMNIC 7 software package (Thermo Electron Corp., Waltham, MA).

SEM and AFM Microscopies. The morphology of the honeycomb films before and after grafting "to" was observed using a atomic force microscope (AFM, Digital Instruments 3000) in tapping mode and a scanning electron microscope (FEI Quanta 200 ESEM) in conventional mode using a low vacuum (0.1−1.0 Torr). The honeycomb was metalized using a gold layer to lead to a conductive sample.

Polymer Synthesis. Synthesis of a tetrafunctional ATRP initiator, 1,2,3,4,6-penta-*O*-isobutyryl bromide-α-D-glucose was implemented according to a method described in the literature.[11]

Synthesis of Polystyrene Stars and Linear by ATRP. Polystyrene stars comprising 5 arms (PSTY-star), and polystyrene linear polymers (PSTY-linear), were synthesized via ATRP using the procedure of Angus et al.[11] Product purity was confirmed using ^{1}H NMR, and the molecular weights were determined by SEC.

polymer	molecular weight M_n	PDI
PSTY-star	69 000	1.10
PSTY-linear	65 000	1.25

Synthesis of Polystyrene Isoporous Films with High Uniformity. A solution comprised of PSTY-stars (20 mg/mL) and PSTY-linear (4 mg/mL) in carbon disulfide was cast onto polypropylene supports under humid conditions to yield honeycomb-patterned membranes.

Surface-Confined Grafting of Glycidyl Methacrylate. Grafting was achieved using the following method: a polymerization stock solution (3 mL) comprised of Bipy (0.64 g, 4.1 mmol), GMA (7.1 g, 50 mmol), and a solvent mixture of distilled water and methanol (20 mL, 1:4 v/v) was added to a vial containing CuBr (26 mg, 0.18 mmol). The vial was immersed in an ultrasonic bath for 15 s to help dissolve the catalyst. The macroporous films on the polypropylene supports were then added to the vials and degassed with nitrogen for 20 min in an ice bath. The polymerizations were conducted at 25 °C and allowed to proceed for a designated reaction time ranging from 30 to 120 min.

After the required polymerization time, the films were removed from the vials and rinsed thoroughly with a methanol/water (1:1 v/v) mixture, followed by a pure methanol wash to remove residual catalyst and monomer.

Epoxide Hydrolysis. The honeycomb membrane consisting of PSTY-*graft*-PGMA (1 h reaction time) was treated with 1 M sulfuric acid at 35 °C overnight. The modified membrane was then extensively rinsed in Milli-Q water and gently dried. A successful hydrolysis was confirmed by ATR-IR.

(Biotinamido)pentylamine Surface Coupling. To the surface of each honeycomb PSTY-*graft*-PGMA membrane a solution comprising of Milli-Q water (0.5 mL) and a (biotinamido)pentylamine solution in DMF (25 μL, 50 mM) was added dropwise, ensuring coverage of the entire membrane. The coupling reaction was allowed to proceed overnight in a humid atmosphere at 25 °C, after which the modified membranes were extensively rinsed with Milli-Q water and gently dried. A successful surface modification was confirmed by ATR-IR.

Strepavidin/Biotin Assay. To the surface of each honeycomb membrane PSTY-*graft*-PGMA a solution comprising of Milli-Q water (0.5 mL) and a Strep-Cy5 solution in DMF (25 μL, 100 μg/mL) was added dropwise until the entire membrane was covered. The assay was allowed to proceed for 1 h at 25 °C in a humid atmosphere, after which the modified membrane was extensively rinsed with Milli-Q water and gently dried. The surface was then examined using fluorescence spectroscopy.

Cell-Growth Studies. The nonmotile, hydrophobic *Psychrobacter* sp. strain, SW5, was cultured in minimal artificial seawater medium (MMM), supplemented with glutamic acid (20 mM) (MMMglt) as a carbon and energy source. The laminar flow slide chambers used were sterilized by autoclaving. Substrata consisted of polypropylene slides with macroporous PSTY-*graft*-PGMA films attached. A control substratum of unmodified macroporous PSTY film was used. Colonisation of the substratum was initiated by inoculating sterile laminar flow chambers with cells grown in the MMMglt liquid culture. The A_{600}s of cultures were determined by and adjusted immediately prior to inoculation to 0.1 by dilution in MMMglt. Slide chambers were inoculated with a single 1.0 mL pulse of SW5 upstream from the chamber under static conditions, and flow was resumed 1 h after the addition of the inoculum. The bulk laminar flow rate was maintained at 2 cm/s throughout the experiments. The bacterium study was carried out at room temperature and was allowed to proceed for 4 days. Positive staining of SW5 cells was achieved by fluorescence inclusion of rhodamine B (0.7 g of rhodamine B per liter in 0.15 M phosphate-buffered saline) and 0.07 M Tris-HCl. The fluorophore (1 mL) was injected upstream of the flow chamber and retained in the chamber by sealing both inlet and outline. Fluorescent images were acquired using an Olympus GB200 scanning confocal microscope.

Results and Discussion

The synthesis of 1,2,3,4,6-penta-*O*-isobutyryl bromide-α-D-glucose was performed according to a published method, and the structure was confirmed via ^{1}H NMR and ^{13}C NMR. There are experimental precedents describing living radical polymerizations of different monomers from functionalized sugar cores utilizing ATRP.[25,53−55] The sugar cores can be selected to bear different levels of functionalization ranging from 5 up to 18 per molecule, yielding star-shaped polymers with different numbers of arms. The number of arms on a star will influence the morphology of films cast using the breath figures method. It has been found that increasing arm numbers yields smaller pores.[29,56,57]

In our work, polystyrene-based films were of interest, as (since the original work of Francois and others) they tend to cast highly uniform films with considerable tolerance to the casting conditions. The syntheses of five-armed polystyrene stars from a glucose core (M_n 69 000 g/mol and PDI 1.10) and linear polystyrene (M_n = 65 000 g/mol and PDI = 1.25) were achieved using established procedures[25] (caution: the MWT of the stars determined by SEC with linear standards are likely to be underestimates of the actual molecular weights[58]). The film casting of PSTY-stars was undertaken

(53) Lia, J.; Xiao, H. *Tetrahedron Lett.* **2005**, *46*, 2227–2229.
(54) Li, J.; Gu, Z.; Xin, J.; Zha, G.; Xiao, H. *Carbohydr. Polym.* **2009**, *79*, 277–283.
(55) Matyjaszewski, K.; Xia, J. *Chem. Rev.* **2001**, *101*, 2921.
(56) Connal, L. A.; Vestberg, R.; Gurr, P. A.; Hawker, C. J.; Qiao, G. G. *Langmuir* **2008**, *24*, 556–562.
(57) Blencowe, A.; Tan, J. F.; Goh, T. K.; Qiao, G. G. *Polymer* **2009**, *50*, 5–32.
(58) Heise, A.; Hedrick, J. L.; Trollsås, M.; Miller, R. D.; Frank, C. W. *Macromolecules* **1999**, *32*, 231.

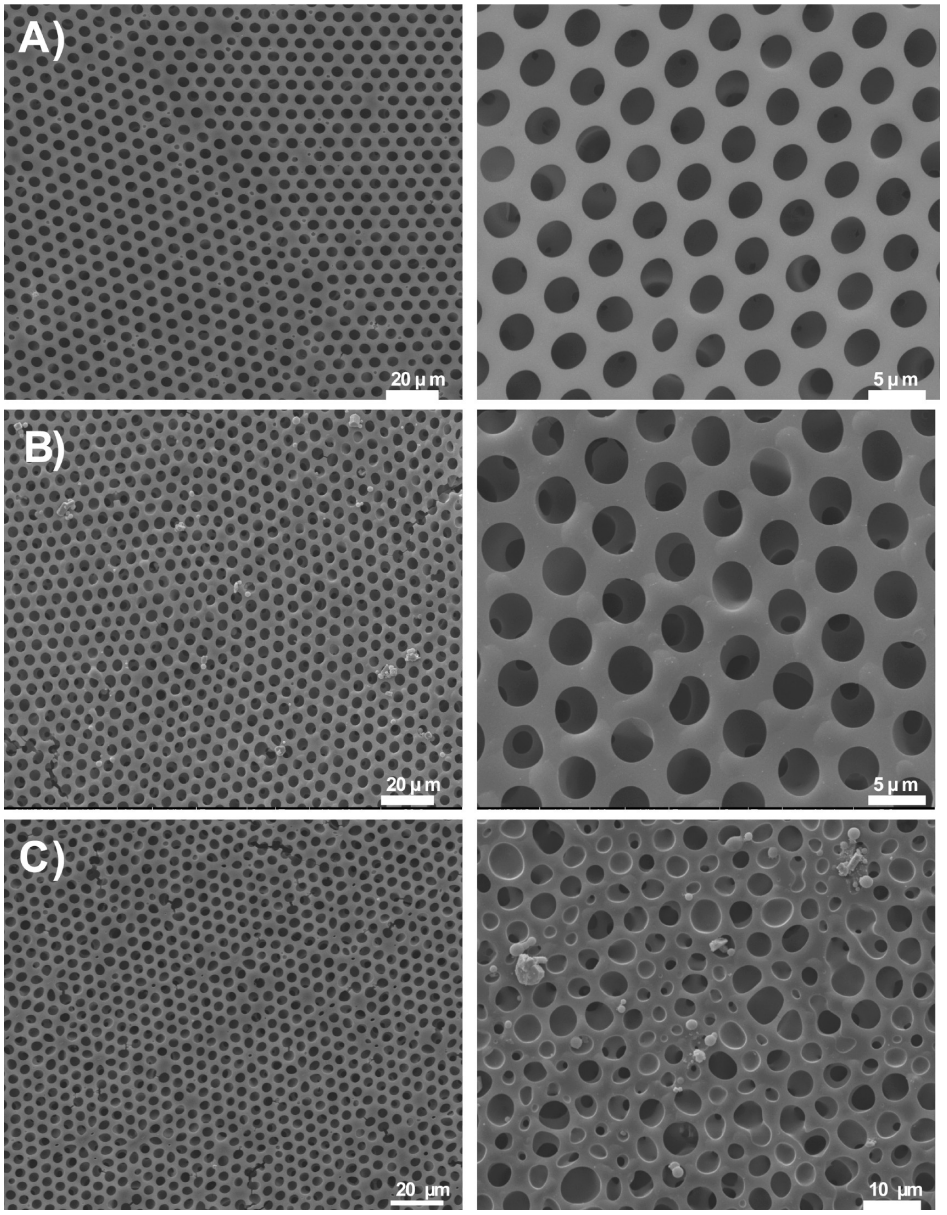

Figure 1. SEM images of (A) PSTY honeycomb film, (B) PSTY-*graft*-PGMA grafted for 30 min, and (C) PSTY-*graft*-PGMA grafted for 120 min.

using a specifically designed casting box, using CS_2 as the casting solvent. A casting box was used to ensure a constant humidity of 75% throughout the film formation process. As published previously,[26] the addition of linear PSTY (M_n = 65 000 g/mol and PDI = 1.25) was necessary to obtain ordered honeycomb patterned films. Images obtained SEM (Figure 1A), optical microscopy (Figure S1), and AFM (Figure S2) clearly revealed a highly uniform hexagonal arrangement of pores in the honeycomb membrane with a diameter of ~3 μm.

Surface Grafting from Isoporous Membranes. The methodology adopted for the graft polymerization of GMA from the surface of isoporous membranes exploited the ATRP end groups present at the end of each star arm (Scheme 1, step 1). Bromine end groups present at the film surface were used to reinitiate further polymerization processes under suitable conditions, as shown by others.[55] An important goal in our experimental protocol was to maintain the uniform honeycomb structure during the grafting process. The morphology of the porous film can be affected by the conditions used for grafting, such as monomer concentration and the choice of solvent.[9,17] Injudicious selection of monomer concentration or solvent will distort or even dissolve the films disrupting the isoporous structure. Since the porous films were not cross-linked or covalently bound to the surface onto which they were cast, the choice of organic solvent for grafting was limited. However, the ease of film dissolution has advantages in analysis because this facilitates film removal and analysis via SEC and NMR.

Surface grafting of PGMA by ATRP under mild conditions has been widely reported.[45,48,59,60] PGMA is a useful and versatile monomer because the epoxide groups can be used for several subsequent coupling chemistry,[61,62] for example, biofunctionalization via attachment of amine functionalized biological molecules, such as peptides, antibodies, and DNA. Alternatively, PGMA can be

(59) Jones, D. M.; Brown, A. A.; Huck, W. T. S. *Langmuir* **2002**, *18*, 1265–1269.
(60) Akkaya, B.; Uzun, L.; Altinta, E. B.; Candan, F.; Denizli, A. *J. Macromol. Sci., Part A* **2009**, *46*, 232–239.
(61) Zemanová, I.; Turková, J.; Čapka, M.; Nakhapetyan, L. A.; Švec, F.; Kálal, J. *Enzyme Microb. Technol.* **1981**, *3*, 229–232.
(62) Zhang, M.; Sun, Y. *J. Chromatogr. A* **2001**, *912*, 31–38.

Scheme 1. Biomimetic Surface Modifications of PSTY Honeycomb Isoporous Membranes

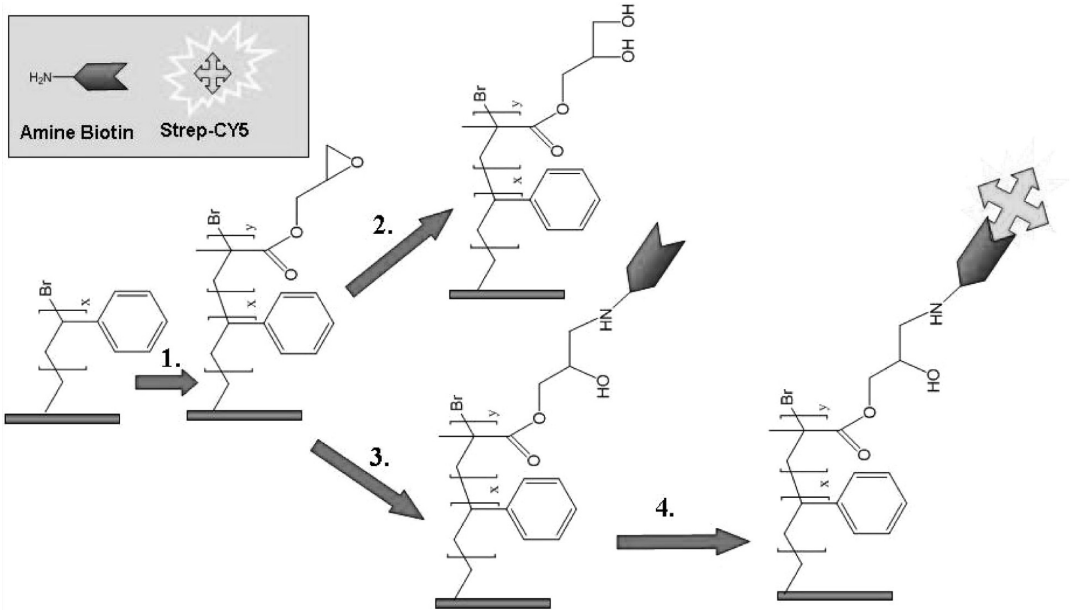

transformed easily into hydrophilic polyglycerol methacrylate via hydrolysis of the epoxide groups into glycerol groups. Our grafting conditions were inspired by the work of Huck et al.,[59] who grafted PGMA onto gold surfaces at 25 °C in a solvent mixture of methanol and water. Our first attempt to graft PSTY with PGMA using the same conditions as Huck et al.[59,63] was unsuccessful because we found that the concentration of monomer had to be lowered (from 50 vol % to ~25 vol %) in order to prevent dissolution of the porous film in the polymerization mixture. The grafting of GMA was performed in aqueous media at room temperature using a CuBr/Bipy catalyst system for time periods up to 2 h (30 min intervals). After the surface grafting, the membranes were rinsed in a water/methanol mixture followed by pure methanol to remove residual catalyst and monomer. The films were then dried and analyzed by nondestructive optical microscopy, to examine changes in the film morphology, and ATR-IR, to confirm the presence of surface-grafted GMA. The changes in morphology of the films caused by different yields of grafted PGMA were determined by SEM (Figure 1B,C), optical microscopy (Figure S1, B and C), and AFM (Figure S2, B). It is evident that large grafting yields were detrimental to the film morphology at longer reaction times (Figure 1C, Figure S1, C), with the pores becoming increasingly distorted either by being filled with grafted material or by being buried under a layer of PGMA. For thick grafted layers, the surface-grafted PGMA layer will also start to swell in the reaction medium, which may also contribute to the distortion of the film morphology as more clearly demonstrated in both the SEM (Figure 1C) and AFM (Figure S2, B) images. Careful examination of the AFM images at high magnification revealed an increase in surface roughness/distortion on grafting, not observed in either the optical or SEM images at lower grafting times, which may be indicative of the surface grafting of GMA chains. However, a more detailed examination was not possible due to the limiting effects of microscopic unevenness of the membrane surface (reflecting the inherent unevenness of the polymer substrate).

ATR-IR analysis confirmed the presence of GMA brushes on the surface of the films (Figure S3). The spectra in Figure S3 were normalized to the PSTY peak at 750 cm^{-1} in order to afford an easy comparison. The main feature of the spectrum demonstrating surface-initiated grafting of PGMA is the appearance of a C═O ester stretch at 1727 cm^{-1}, resulting from the ester groups present in PGMA. There is also an increase in the relative intensity of the glycidyl bands at 905 and 842 cm^{-1}, coincident with PSTY bands associated with monosubstituted phenyl groups.

To quantify GMA surface grafting, the films were analyzed by both SEC and NMR. This required the solubilization of the films in appropriate solvents. The ^1H NMR spectrum after grafting is shown in Figure S4. All the signals in the spectra could be uniquely identified as belonging to either the PSTY or PGMA components. The signal designated with an asterisk (Figure S4) is assigned to the ring-opening of the epoxide group caused by coordination of Cu(I) followed by a reaction with methanol to yield methoxy groups as a side reaction during the surface grafting procedure. Additional experiments were carried out with lower amounts of CuBr in order to verify this assumption. It was evident from the NMR characterization that the use of lower concentrations of CuBr indeed resulted in a reduction of this signal (data not shown).

Quantification of the NMR peaks provided evidence of the surface grafting of GMA. Analysis of the ratio of signal 3 (phenyl group 5H) in the PSTY block and signal 6 (CH_2− side-chain group) in the PGMA block plotted against reaction time is shown in Figure 2A. The amount of grafted PGMA increased in a nonlinear fashion with time. The growth profile indicates that the rate of polymerization increased with time, reflecting a change in the surface characteristics as grafting proceeded. In the early stages of grafting, the surface is hydrophobic, limiting access of the bromine end groups to the hydrophilic solution of water, methanol, GMA, and catalyst. As grafting proceeds, the bromine end groups become anchored to growing PGMA chains and much more accessible to the GMA monomer in solution.

SEC analysis confirmed a slight increase in the molecular weight of the polymers, in accord with the surface grafting of GMA (Figure 2B). Further analysis is complicated by the fact that not all arms on a given PSTY star will be equally accessible to chain extension. As surface grafting proceeds, the interface changes, and more star arms may become "visible" to the grafting solution. Also, the RI detector available is about 4 times more sensitive to the PSTY component (cf. the grafted PGMA component due

(63) Jones, D. M.; Huck, W. T. S. *Adv. Mater.* **2001**, *13*, 1256–1259.

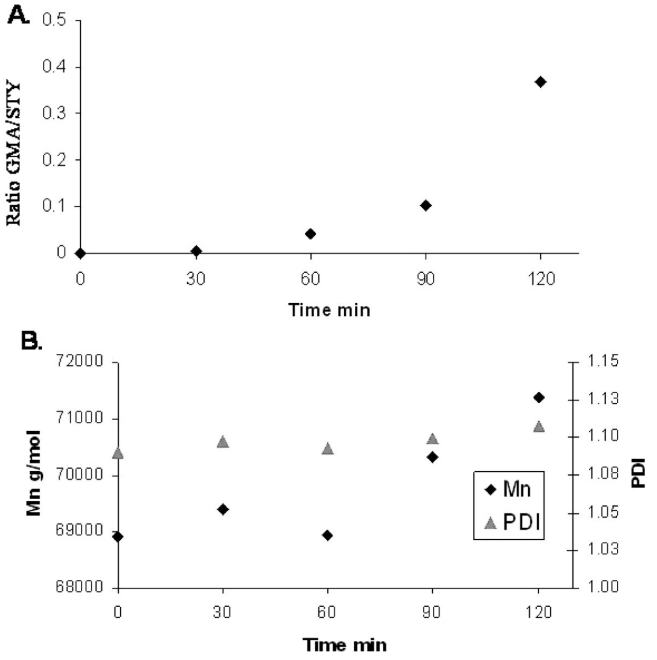

Figure 2. Analysis of GMA surface grafting on PSTY honeycomb films by (A) ^{1}H NMR and (B) SEC analysis.

to the significant differences in their respective d*n*/d*c* values), thus reducing the quantitative nature of the SEC data. Typical SEC traces for the neat and grafted membranes are presented in Figure S5.

To confirm that free PGMA was not formed in the supernatant of the grafting solution (and therefore adsorb to, rather than graft from, the membrane), a control experiment was also performed. A grafting solution was prepared (as described in the Experimental Part), degassed, and allowed to polymerize for 120 min at 25 °C—conditions under which the surface grafting was performed. Samples were taken periodically, concentrated, and subject to analysis by SEC. In all samples the presence of solution polymerized PGMA could not be detected. Further, we found that we could not efficiently reinitiate GMA from the surface of films that were not cast to give honeycomb films. We attributed this to the effect of preferential partitioning of the living chain ends at the interface between the water droplet and polymer solution, as the film is formed. This effect has been previously demonstrated in the work of Stenzel et al.[26] Therefore, the isoporous nature is essential for the successful and controlled grafting-from approach demonstrated here.

Membrane−Bacterial Interactions. The nonmotile *Psychrobacter* sp. strain, SW5, was used to investigate the hydrophobic nature of the grafted macroporous films at a micrometer level, rather than the millimeter level as typically detected by water contact angle measurements. The growth morphology of this bacterium is known to change, in a predictable way, in response to changes in the hydrophilic−hydrophobic balance of the growth substrate. We therefore used this bacterium as a *biological probe* to confirm our surface grafting process was successful and also investigate the surface graft coverage because these will change the hydrophobic character of the surface. Using a biological probe in parallel with the more widely used instrumental method of surface characterization, e.g., ATR-IR, gives further insight into the possible use of these materials in applications where they come into contact with living cells, such as coatings for implants or substrates for cell growth. Also, the efficiency of the rinsing procedure for the removal of copper after the grafting of PGMA

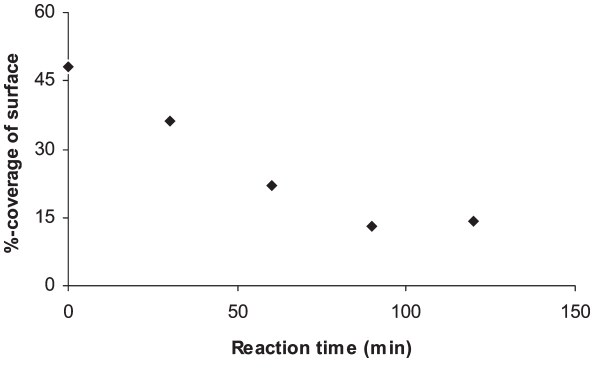

Figure 3. Surface coverage of bacteria on PSTY and PSTY-*graft*-PGMA honeycomb films as a function of grafting time, determined by fluorescent image analysis.

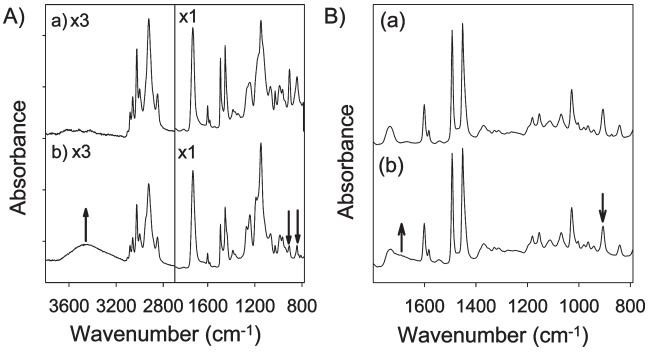

Figure 4. ATR-IR spectra of PSTY-*graft*-GMA macroporous films with (A) epoxide hydrolysis, before, and (B) reaction with aminobiotin, before (a) and after (b).

was verified as copper is known to poison living cells.[64] The PSTY films (as a reference sample) and PSTY-*graft*-PGMA surfaces (Figure S6) were colonized with the SW5 bacteria. The hydrophobic PSTY surfaces exhibited bacterial colonies characterized by the formation of packed biofilms consisting of single and paired cells (Figure S6A). The results are in accord with previous studies, as the SW5 bacteria show a high affinity for hydrophobic surfaces.[65]

In contrast, the SW5 bacteria sparsely colonize the less hydrophobic PSTY-*graft*-PGMA surfaces favoring the formation of chains (Figure S6, B and C) consistent with the bacteria attempting to minimize contact with the surface. Bacteria growth plotted versus grafting time of PGMA time is shown in Figure 3, showing that the cell growth decreases with reaction time (greater PGMA grafting), indicating that the surfaces become less hydrophobic with a greater coverage of grafted PGMA.

Epoxide Hydrolysis. The pendant epoxide groups in PGMA were used for further modification. The honeycomb membrane, consisting of PSTY-*graft*-PGMA, was treated with 1 M sulfuric acid at 35 °C overnight, followed by extensive rinsing with water (Scheme 1, step 2). Figure 4 shows the PSTY star-*graft*-PGMA before (a) and after (b) acid treatment. The formation of hydroxyl groups is clearly seen using ATR-IR spectra (a broad absorption at 3400 cm^{-1}). Furthermore, decreases in the absorptions at 906 and 842 cm^{-1} are observed, consistent with a reduction in epoxide functionality. PSTY also has absorptions that overlap in this spectral region (vide infra). As PSTY remains unaffected by acid

(64) Nawaz, M.; Manzl, C.; Krumschnabel, G. J. *Bull. Environ. Contam. Toxicol.* **2005**, *75*, 652–661.
(65) Dalton, H. M.; Stein, J.; March, P. E. *Biofouling* **2000**, *15*, 83.

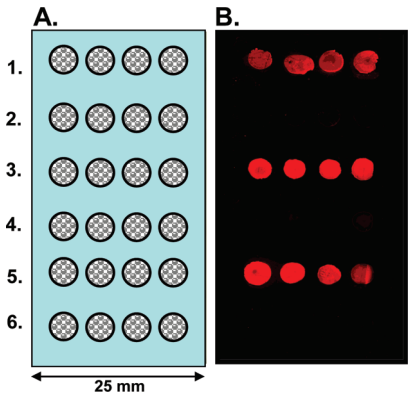

Figure 5. Fluorescent images of biotinylated biomimetic surfaces probed with STREP-CY5: membrane map (A) and fluorescent image (B) (rows 2, 4, and 6: control; rows 1, 3, and 5: biotinylated).

treatment, the absorptions in this region (attributable to PSTY) will remain unaffected. ^{1}H NMR analyses to confirm the formation of OH groups proved unsuccessful as the modified films were difficult to fully solubilize, as the amphiphilic blocklike structure and possible intermolecular cross-linking (self-polymerization) events between liberated hydroxyl groups and intact epoxides both cause solubility problems.

Construction of a Biomimetic Surface. The epoxide functionally of the polyGMA grafted surface chains is a very versatile synthetic handle that can couple in a "click-like" fashion to a variety of suitably functional (including alcohols, thiols, carboxylic acid, and amine groups) terminated biorelevant molecules (e.g., peptide, proteins, DNA, or RNA) to create a biomimetic surface. To demonstrate this, we made use of the epoxide group to couple a model amine functional biomolecule, amino-functionalized biotin, to the surface, thus creating (biotinamido)pentylamine-functionalized surface (Scheme 1). (Biotinamido)pentylamine has a reactive amine group that can react with the pendant epoxides under mild conditions (Scheme 1, step 3). A 4×6 array of isoporous films was cast onto a PFA, a perfluoropolymer, film (Figure 5A). This membrane array is shown as a diagram in Figure 5A.

PFA is highly resistant to nonspecific protein binding and also found to exhibit a low fluorescent background for an excitation wavelength of 650 nm. This array was then subjected to the same surface grafting conditions discussed above to form surface-confined PGMA brushes (1 h reaction) on each film of the array. The films were then derivatized with (biotinamido)pentylamine. The success of this modification was confirmed by the appearance of the amide I band at 1647 cm^{-1} characteristic of the urea from the biotin moiety in the FTIR-ATR spectrum (Figure 4B). A small decrease was also observed in the epoxide band at 906 cm^{-1}, which indicated that the coupling occurred through reaction with epoxide groups. However, a significant number of epoxides remained unreacted. To minimize nonspecific binding of Cy5-labeled streptavidin to the substrates, all membranes on the array were blocked by incubating with bovine serum albumin (BSA) at 37 °C for 30 min in a humid environment. Unbound BSA was removed by thorough rinsing of the substrates with Milli-Q water.

To further investigate the presence of the biotinylated and nonbiotinylated PSTY-*graft*-PGMA honeycomb films were both probed using a fluorescently labeled streptavidin probe (Strep-Cy5: Scheme 1, step 4). Biotin is well-known to specifically bind to streptavidin via strong small molecule−protein binding events. This not only allows the success of the model surface modification to be assessed but also, importantly, demonstrates the possible use of these modified honeycomb membranes in a model enzyme-linked immunosorbent sandwich assay (ELISA).

The fluorescence images confirm the presence of the biotin/Strep-Cy5 conjugate (odd rows, Figure 5B) while only low levels of autofluorescence are discernible for the control surface (even rows, Figure 5B).

Conclusion

Experimental conditions for the successful surface modification of honeycomb films have been identified. The integrity of the porous films could be maintained while epoxide-containing surface grafts, PGMA, were covalently attached. The versatility of the epoxide functionality for further surface modification was demonstrated via acid hydrolysis to form a hydroxylated surface and the biofunctionalization using (biotinamido)pentylamine functionalization. The success of these modifications was confirmed by both spectroscopic and biological means.

Acknowledgment. The research performed at CAMD on honeycomb polymer films from breath figures was funded by a 5 years Discovery Grant (DP0208414) and an Australian Professorial Fellowship both awarded to TPD by the Australian Research Council (ARC). We also acknowledge Linkage funding from the ARC on a joint project with Polymerat PTY Ltd. (AKA Biolayer). This work was also supported in part by DP0878615 (held by I.B.). We thank Dr. Helen Dalton, Dr. Jenny Norman, and Dr. Katie Levick for assistance with bacterial growth experiments and confocal microscopy, SEM, and AFM, respectively, and the UNSW electron microscopy unit.

Supporting Information Available: Figures S1−S6. This material is available free of charge via the Internet at http://pubs.acs.org.